medRxiv preprint doi: https://doi.org/10.1101/2021.03.02.21252754; this version posted January 13, 2022. The copyright holder for this preprint (which was not certified by peer review) is the author/funder, who has granted medRxiv a license to display the preprint in perpetuity. It is made available under a CC-BY-NC-ND 4.0 International license .

Redesigning SARS-CoV-2 clinical RT-qPCR assays for wastewater RT-ddPCR

Raul Gonzalez[a*], Allison Larson[a], Hannah Thompson[a], Errin Carter[a], Xavier Fernandez Cassi[b]

[a]Hampton Roads Sanitation District, 1434 Air Rail Avenue, Virginia Beach, VA, 23455, United States

[b]École Polytechnique Fédérale de Lausanne (EPFL), CH-1015 Lausanne, Switzerland

*Corresponding author, rgonzalez@hrsd.com, ORCID 0000-0002-8115-7709

Keywords

SARS-CoV-2

Droplet Digital PCR

Wastewater

Wastewater-based Epidemiology

Wastewater Surveillance

Declarations

Funding: no external funding was received

Conflicts of interest/competing interests: none

Availability of data and material: This manuscript has data included as supplemental information. Additional data will be made available on reasonable request.

medRxiv preprint doi: https://doi.org/10.1101/2021.03.02.21252754; this version posted January 13, 2022. The copyright holder for this preprint
(which was not certified by peer review) is the author/funder, who has granted medRxiv a license to display the preprint in perpetuity.
It is made available under a CC-BY-NC-ND 4.0 International license .

Abstract

COVID-19 wastewater surveillance has gained widespread acceptance to monitor community infection trends. Wastewater samples primarily differ from clinical samples by having low viral concentrations due to dilution, and high levels of PCR inhibitors. Therefore, wastewater samples should be processed by appropriately designed and optimized molecular workflows to accurately quantify targets. Digital PCR has shown to be more sensitive and resilient to environmental matrix inhibition. However, most SARS-CoV-2 assays have been designed for clinical use on RT-qPCR instruments, then adopted to digital PCR platforms. But it is unknown whether clinical RT-qPCR assays are adequate to use on digital PCR platforms. Here we designed an N and E gene multiplex (ddCoV_N and ddCoV_E) specifically for RT-ddPCR and benchmarked them against the nCoV_N2 and E_Sarbeco assays. ddCoV_N and ddCoV_E have equivalent limits of detections and wastewater sample concentrations to NCoV_N2 and E_Sarbeco but showed improved signal-to-noise ratios that eased interpretation and ability to multiplex. From GISAID downloaded unique sequences analyzed, 2.12% and 0.83% present a mismatch or would not be detected by the used primer/probe combination for the ddCoV_N and ddCoV_E, respectively.

medRxiv preprint doi: https://doi.org/10.1101/2021.03.02.21252754; this version posted January 13, 2022. The copyright holder for this preprint
(which was not certified by peer review) is the author/funder, who has granted medRxiv a license to display the preprint in perpetuity.
It is made available under a CC-BY-NC-ND 4.0 International license .

Introduction

Globally there have been over 83,000,000 cases and 1,800,000 deaths due to the coronavirus disease-2019 (COVID-19) pandemic in 2020 alone (Dong et al., 2020). Wastewater surveillance of severe acute respiratory syndrome coronavirus 2 (SARS-CoV-2), the virus that causes COVID-19, has been used as an epidemiological tool to better understand the infection extent in sewershed communities (e.g. Gerrity et al., 2021; Gonzalez et al., 2020; Prado et al., 2021; Randazzo et al., 2020; Hata et al. 2021; Carrillo-Reyes et al., 2020).

Two main differences exist between clinical and environmental samples. First, environmental samples typically have lower viral concentrations compared to clinical (e.g., nasopharyngeal, throat, stool, sputum) samples. This is primarily due to dilution effects and often require environmental samples to be concentrated prior to quantification. Second, environmental matrices can have a wide variety of inhibitory substances that are co-concentrated in environmental workflows. Thus, environmental samples require molecular workflows that have properly designed and optimized assays to maximize sensitivity and accuracy. An appropriate assay design reduces primer dimers that can interfere with accurate quantification, which is especially important at lower concentrations. Additionally, proper assay design and optimization can improve signal-to-noise ratios that can facilitate interpretation of true positives. The signal-to-noise ratio is especially important to certain digital PCR platforms (i.e., droplet digital PCR).

medRxiv preprint doi: https://doi.org/10.1101/2021.03.02.21252754; this version posted January 13, 2022. The copyright holder for this preprint (which was not certified by peer review) is the author/funder, who has granted medRxiv a license to display the preprint in perpetuity. It is made available under a CC-BY-NC-ND 4.0 International license .

Reverse transcription-qPCR (RT-qPCR) and RT-digital PCR have been the dominant molecular methods used to quantify SARS-CoV-2 in wastewater (e.g., Pecson et al., 2021; Fores et al., 2021; Oliveira et al., 2020; Cervantes-Aviles et al., 2021; Alygizakis et al., 2021; Torii et al., 2021). Many RT-qPCR SARS-CoV-2 assays have been developed for various genome regions—N gene, E gene, S gene, etc. (Lu et al., 2020; Corman et al., 2020; Chu et al., 2020; China CDC, 2020). These assays have been designed based on general RT-qPCR specifications and some have design faults from not strictly following design guidelines. However, these assays can still provide adequate quantification, even without strict adherence to recommended design specifications, because of high titer clinical samples. Digital PCR has been proven to be more sensitive than qPCR (Falzone et al., 2020; Liu et al., 2020; Suo et al., 2020), especially in environmental matrices (Graham et al., 2021; Cao et al., 2015; Yang et al., 2014; Racki et al., 2014), with some exceptions (e.g., D'Aoust et al., 2021). The assays used have all been designed for clinical use on RT-qPCR instruments, then adopted to digital PCR platforms. Some digital PCR platforms, like droplet digital PCR (ddPCR), require a stricter adherence to assay design criterion since the technology relies on the clear separation of positive and negative droplets or partitions.

Early on in the SARS-CoV-2 pandemic the following knowledge gap has been identified: Are clinical RT-qPCR assays adequate to use on digital PCR platforms, especially when analyzing environmental samples that have strong matrix inhibition and are subject to dilution effects? Here we designed and optimized a SARS-CoV-2 RT-ddPCR multiplex for wastewater following strict design criteria to maximize accuracy especially at the lower concentrations in a difficult

medRxiv preprint doi: https://doi.org/10.1101/2021.03.02.21252754; this version posted January 13, 2022. The copyright holder for this preprint (which was not certified by peer review) is the author/funder, who has granted medRxiv a license to display the preprint in perpetuity. It is made available under a CC-BY-NC-ND 4.0 International license .

matrix (wastewater). N and E gene assays were specifically designed for ddPCR and compared to the nCoV_N2 and E_Sarbeco assays (Lu et al., 2020; Corman et al., 2020) designed for RT-qPCR. Knowing the effect of strict adherence to digital PCR design specifications is necessary since wastewater surveillance has seen a shift from trend analysis at the sewershed scale to finer resolution building level screening of individuals. Thus, pushing the need for an appropriately optimized method for environmental samples.

Methods

Assay Design. Many COVID-19 wastewater surveillance researchers have been running multiple assays for the same gene (e.g., Sherchan et al., 2020, Medema et al., 2020; Ahmed et al., 2020). This is highly redundant and not normally done in wastewater studies quantifying pathogens (e.g., Worley-Morse et al. 2019; Sarmila et al., 2020). A better strategy to gain higher confidence of results would be to quantify multiple conserved genes in the virus. We have designed 2 assays targeting N and E genes using Primer3Plus software (Untergasser et al., 2007) and the criteria found in Supplemental Table S1. In short, we strictly followed widely accepted PCR design criteria (and specific manufacturer recommendations) to lower primer dimer scores, and target recommended GC content (40-60%), melting temperatures (Tm; 60-63°C for primers, 4-6°C higher for probes), and lengths. The newly designed primers and probes for RT-ddPCR (ddCoV_N, ddCoV_E) can be seen in Table 1. Optimization and validation of these assays was done alongside the popularly used nCoV_N2 and E_Sarbeco assays. Geneious Prime (Geneious Biologics, Auckland, New Zealand) was used to visualize the newly designed primer and probe

medRxiv preprint doi: https://doi.org/10.1101/2021.03.02.21252754; this version posted January 13, 2022. The copyright holder for this preprint (which was not certified by peer review) is the author/funder, who has granted medRxiv a license to display the preprint in perpetuity. It is made available under a CC-BY-NC-ND 4.0 International license .

104 positions with respect to the nCoV_N2 and E_Sarbeco assays. Primer3Plus Primer_Check task
105 (with the conditions in Supplementary Table S1) was used to determine the primer and probe
106 Tm, GC content, and affinity for self-complementarity (likelihood that a primer will bind to itself
107 or the other primer).
108
109 *Sample Concentration and RNA Extraction.* Wastewater concentration was done using
110 electronegative filtration according to Gonzalez et al. (2020). In short, $MgCl_2$ was added to a
111 final concentration of 25 mM to 25 - 50 mL wastewater, then acidified to a pH of 3.5 with 20%
112 HCl. The sample was then filtered through a mixed cellulose ester HA filter (HAWP04700;
113 Millipore, Billerica, MA, USA). A total of $1.0x10^6$ copies of bovine coronavirus (CALF-GUARD;
114 Zoetis, Parsippany, NJ) was added to all samples prior to filtration to determine total process
115 recovery. Bovine coronavirus recovery using RT-ddPCR (Gonzalez et al., 2020) was the ratio of
116 bovine coronavirus sample concentration to spike concentration.
117
118 Filters were immediately stored in a -80°C freezer until RNA extraction on a NucliSENS easyMag
119 (bioMerieux, Inc., Durham, NC, USA) within 5 days of filtration. Extractions were preformed
120 using a modified manufacturer's protocol B 2.0.1. Modifications included a 30-min off board
121 lysis (2 mL of lysis buffer) and 100 µL of magnetic silica beads to minimize matrix inhibition and
122 maximize RNA recovery.
123
124 *Reverse Transcription Droplet Digital PCR.* Digital PCR workflow used the one-step RT-ddPCR
125 advanced kit for probes on the Bio-Rad QX200 (Bio-Rad, Hercules, CA, USA). The 20 µL final

medRxiv preprint doi: https://doi.org/10.1101/2021.03.02.21252754; this version posted January 13, 2022. The copyright holder for this preprint (which was not certified by peer review) is the author/funder, who has granted medRxiv a license to display the preprint in perpetuity. It is made available under a CC-BY-NC-ND 4.0 International license .

126 reaction volume consisted of the following: 5 µL 1 × one-step RT-ddPCR Supermix (Bio-Rad), 2
127 µL reverse transcriptase (Bio-Rad), 1 µL 300 mM DTT, 3 µL of forward and reverse primers (900
128 nM final concentration) and probes (250 nM final concentration), 5 µL RNase-free water, and 4
129 µL RNA (samples run undiluted). The 20 uL volume was combined with 70 µL droplet generation
130 oil in the Droplet Generator (Bio-Rad) and resulting droplets were transferred to a 96-well plate
131 for end-point PCR. PCR cycling conditions were: 60-min reverse transcription at 50°C (1 cycle),
132 10-min enzyme activation at 95°C (1 cycle), 30-s denaturation at 94°C (40 cycles), 1-min
133 annealing/extension cycle at 55°C (40 cycles; ramp rate of ~2–3°C/s), 10-min enzyme
134 deactivation at 98°C (1 cycle) and a hold at 4°C until read on the droplet reader. Positive and
135 negative droplet reading occurred on the Bio-Rad Droplet Reader.
136
137 *Thermal Gradient Optimization.* Optimizing the annealing temperature of a PCR assay is critical,
138 especially for target specificity. The C1000 Thermal Cycler (Bio-Rad) was used to test the
139 reaction across a range of temperatures (60 to 50°C). The Twist Synthetic SARS-CoV-2 RNA
140 Control 4 (part no. 102862; Twist Bioscience, San Francisco, CA, USA) and a SARS-CoV-2 positive
141 wastewater sample was used for the optimization. This optimization also gives the first
142 visualization at the assay efficiency and robustness.
143
144 *Limits of Detection.* Theoretical limits of detection (LOD) were calculated by running serial
145 dilutions of the Twist Synthetic SARS-CoV-2 RNA Control 4 (Twist Bioscience, San Francisco, CA,
146 USA) standard in 10 replicates over 4 orders of magnitude. The LOD was the concentration
147 (copies/reaction) at which over 60% of the technical replicates were positive (Gonzalez et al.,

medRxiv preprint doi: https://doi.org/10.1101/2021.03.02.21252754; this version posted January 13, 2022. The copyright holder for this preprint (which was not certified by peer review) is the author/funder, who has granted medRxiv a license to display the preprint in perpetuity. It is made available under a CC-BY-NC-ND 4.0 International license .

2020). Coefficient of variations (CV) were calculated for the copies per reaction for the serial dilutions to compare replicates at different positive droplet concentrations.

In-silico specificity and primer/probe mismatch analysis. BLASTn (Altschul et al., 1990) was used to test the in-silico specificity of the ddCoV_N and ddCoV_E primers against viruses (taxid: 10239) and bacteria (taxid: 2) in the nr database. There were no BLAST hits presenting good homology and coverage for the primer/probe combinations that suggests assay detection to viruses or bacteria other than SARS-CoV-2.

A total of 105,268 SARS-CoV-2 sequences retrieved and downloaded from GISAID on 06/02/2021 were evaluated in silico for the primer/probes designed. The inclusion criteria for these sequences to be tested in silico were: 1) uploaded sequences from the United States of America on date 01/01/2020 to 31/12/2020; 2) worldwide uploaded sequences from 01/01/2021 to 06/02/2021; 3) only those who have been sequenced from a human host and the collection date is included; 5) only fully completed SARS-CoV-2 genomes from all clades and lineages presenting high coverage were included, low coverage genomes were excluded. Briefly, sequences were imported in Geneious Prime (Geneious Biologics) and duplicated sequences with identical names were removed. Using Geneious software, newly designed primers/probes for the nucleocapsid protein (ddCoV_N) and the envelope gene (ddCoV_E) were mapped using Geneious primer mapper against the retrieved sequences allowing a maximum of 3 mismatches. Sequences with more than three mismatches are summarized in Supplemental Figure S1 and could be considered unlikely to be detected by the tested assay. A

medRxiv preprint doi: https://doi.org/10.1101/2021.03.02.21252754; this version posted January 13, 2022. The copyright holder for this preprint
(which was not certified by peer review) is the author/funder, who has granted medRxiv a license to display the preprint in perpetuity.
It is made available under a CC-BY-NC-ND 4.0 International license .

list of complete mismatches and the relative position within SARS-CoV-2 genome are presented in Supplemental Table S2.

Concentration Comparison. Concentration comparison of the two new assays, nCoV_N2, and E_Sarbeco assays was done on 3 weeks of wastewater samples from 9 different facilities (N=27). These facilities and the collection scheme are described in Gonzalez et al. (2020). Within gene assays concentrations were compared using percent difference.

Results and Discussion

Assays and Performance. The newly designed primers and probes (ddCoV_N and ddCoV_E) are adjacent to the respective nCoV_N2 and E_Sarbeco assay locations. Figure 1 documents the shift in primers and probes necessary to strictly meet widely accepted PCR design criteria and specific manufacturer recommendations (Supplemental Table S1). The information for the two newly designed RT-ddPCR primers and probes as well as the nCoV-N2 and E_Sarbeco assays are in Table 2. The nCoV_N2 and E_Sarbeco assays have high self-complementarity scores in the forward primers. The newly designed assays reduced this score as well as restricted within assay primer/probe Tm differences and constricted the GC%.

The annealing temperature thermal gradients give the first look at the efficiencies of the 4 assays on the QX200 ddPCR platform (Figure 2). With respect to the N gene assays, ddCoV_N created a superior separation between positive and negative droplets for both the high titer

medRxiv preprint doi: https://doi.org/10.1101/2021.03.02.21252754; this version posted January 13, 2022. The copyright holder for this preprint (which was not certified by peer review) is the author/funder, who has granted medRxiv a license to display the preprint in perpetuity. It is made available under a CC-BY-NC-ND 4.0 International license .

192 standard and wastewater sample. Positive droplet amplitude was approximately 10000 for both
193 assays, while the negative droplet band was approximately 500 and 6500 for ddCoV_N and
194 nCoV_N2, respectively. Additionally, the baseline for the ddCoV_N assay was significantly
195 tighter. During the annealing temperature optimization, droplets in the ddCoV_N negative
196 amplitude ranged from approximately 0 to 1000. The droplets in the nCoV_N2 ranged from
197 approximately 500 to 7000. In the wastewater samples, 'raininess' was diminished with the
198 ddCoV_N assay. During the optimization, the E gene assays did not have as significant
199 difference in band amplitudes. The E_Sarbecco amplitude difference was slightly greater than
200 that of the ddCoV_E. E_Sarbeco ranged from approximately 6500 to 11500, while the ddCoV_E
201 ranged from approximately 1600 to 4600. However, the ddCoV_E gene had a noticeably tighter
202 negative baseline—approximately half of the E_Sarbeco assay.
203
204 The increased droplet band separation of the ddCoV_N assay and the tighter negative bands
205 allows for greater ease in interpretation of results. Manual placement of the threshold is
206 difficult with a small gap between positive and negative bands. This can be exacerbated with
207 the 'raininess' caused by partial fluorescence and loose bands. These favorable characteristics
208 are also essential to multiplexing assays. The increased separation and reduction in 'raininess'
209 are likely in part due to the elimination of the BHQ (LGC Biosearch Technologies, Risskov,
210 Denmark) quencher. While recommended by the manufacturer for the instrument, Bio-Rad has
211 advised against the use of BHQ probes (LGC Biosearch Technologies) with their one-step
212 reverse transcription kits since it contains Dithiothreitol (DTT). DTT is thought to cleave BHQ
213 (LGC Biosearch Technologies) when not intended, causing fluorescence clusters. It is unlikely

medRxiv preprint doi: https://doi.org/10.1101/2021.03.02.21252754; this version posted January 13, 2022. The copyright holder for this preprint
(which was not certified by peer review) is the author/funder, who has granted medRxiv a license to display the preprint in perpetuity.
It is made available under a CC-BY-NC-ND 4.0 International license .

that the ZEN/Iowa Black FQ (Integrated DNA Technologies, Coralville, Iowa) double quenched probes alone caused the tighter baselines since the BHQ (LGC Biosearch Technologies) probes used for the nCoV-N2 and E_Sarbeco probes were also double quenched BHQnova (LGC Biosearch) probes.

Limits of Detection. The LODs were nearly identical for each pair of gene assays but almost an order of magnitude different across genes. The N gene LODs were 2.16 and 2.14 copies per reaction for the ddCoV_N and nCoV_N2 assays, respectively. The E gene LODs were 16.0 and 15.0 copies per reaction for the ddCoV_E and E_Sarbeco assays, respectively. Figure 3 shows ddCoV_N and ddCoV_E number of positive droplets and the copies per reaction for the serial dilutions used to calculate the LODs. Coefficients of variation for the replicates were computed using the copies per reaction data for each dilution. For both assays the CV increased through the dilution series but took a large increase at the LODs. The CV increased faster in the ddCoV_E, than the ddCoV_N assay, reflecting the higher LOD.

In-Silico Analyses. From the total of unique sequences analysed, 869 out of 105,227 (0.83%) present a mismatch or would not be detected by the used primer/probe combination for the E gene (ddCoV_E). For E gene assay, most of the mutations affected the designed probe (55%) and the forward primer (35%).

For the in-silico testing of ddCoV_N assay, the total number of sequences analysed was reduced as the retrieved GISAID sequences presented ambiguous basecalls at the Nucleocapsid region.

medRxiv preprint doi: https://doi.org/10.1101/2021.03.02.21252754; this version posted January 13, 2022. The copyright holder for this preprint (which was not certified by peer review) is the author/funder, who has granted medRxiv a license to display the preprint in perpetuity. It is made available under a CC-BY-NC-ND 4.0 International license .

This was not observed for the E gene and it is likely that these ambiguities are related to a high mutation rate on this specific genome site or the fact that the N gene is located at the 3' of SARS-CoV-2 genome. These ambiguities produced false positive results on the primer/probe mapping, significantly increasing the percentage of mismatches detected. Therefore, from the initial 105,227 sequences, a trimming on the sequences on the 3' was applied when more than 40 continuous ambiguous base call were found. As a result of this, some sequences were significantly shortened and only genomes longer than 28Kbs bases were included in the in-silico test for the ddCoV_N. This reduced the total initial sequences analysed to 89,566. From the total of sequences included, 1901 (2.12%) presented a mismatch or would not be detected by the designed assay (more than 3 mismatches). Most of the identified mismatches (1901) affected the probe (47%) or the primer forward (41.6%) targeting the N-gene.

Concentration Comparison. For three weeks the wastewater of 9 major facilities was analyzed using all 4 assays (Figure 4). Bovine coronavirus recoveries for the samples ranged from 0.38% to 19%, with a mean (SD) of 6.6% (4%). These recoveries are in line with previously reported recoveries for the same virus and workflow used (Gonzalez et al., 2020). The detectable concentrations across all assays ranged from $7.00x10^{1}$ to $2.21x10^{4}$ copies/100 mL. One sample was non-detect for all assays. Specifically, the mean (SD) detections for ddCoV_N and nCoV_N2 assays were $4.67x10^{3}$ ($3.60x10^{3}$) and $5.46\ x10^{3}$ ($4.42\ x10^{3}$), respectively. The mean (SD) detections for ddCoV_E and E_Sarbeco assays were $1.94\ x10^{3}$ ($1.46\ x10^{3}$) and $1.92\ x10^{3}$ ($1.49\ x10^{3}$), respectively. The mean (SD) percent difference for detections (N=26) using the N assays was 12 (19). The mean percent difference between the E gene assays was 7 (32). Differences

medRxiv preprint doi: https://doi.org/10.1101/2021.03.02.21252754; this version posted January 13, 2022. The copyright holder for this preprint (which was not certified by peer review) is the author/funder, who has granted medRxiv a license to display the preprint in perpetuity. It is made available under a CC-BY-NC-ND 4.0 International license .

within gene assays was small as expected since the assays were designed around the same genomic locations. The 2-D plot (Figure 5) highlights the assays multiplexing performance for the first 9 samples analyzed. There is clear clustering of the droplet populations—gray = double negative, blue = FAM positive, green = HEX positive, and orange = double positive. The optimized, newly designed assays translate well to multiplexing and easily interpretable results.

Conclusion

SARS-CoV-2 wastewater surveillance has been practiced widely to examine community level infection trends and even to screen for infected individuals at the building level. Wastewater SARS-CoV-2 concentrations can be significantly lower than clinical samples due to dilution and environmental RNA degradation. Because of this well designed and optimized molecular assays should be used in environmental sample workflows. The ddCoV_N and ddCoV_E assays have been designed to lower dimer scores and strictly follow PCR design guidelines, specifically those recommended for ddPCR. While the RT-ddPCR assays have equivalent LOD and concentrations, they have improved signal-to-noise ratios that ease interpretation and decrease the likelihood of false positives due to misinterpretation. This is especially important for novice users and ultimately this improved efficiency is translated to an easier ability to multiplex. *In-silico* analysis of the designed primers and probes should be periodically conducted to ensure continued assay appropriateness in SARS-CoV-2 environmental monitoring. New variants are constantly emerging with mutations affecting the targeted genes which ultimately can decrease the sensitivity of currently used assays.

medRxiv preprint doi: https://doi.org/10.1101/2021.03.02.21252754; this version posted January 13, 2022. The copyright holder for this preprint (which was not certified by peer review) is the author/funder, who has granted medRxiv a license to display the preprint in perpetuity. It is made available under a CC-BY-NC-ND 4.0 International license .

References

Ahmed, W., Angel, N., Edson, J., Bibby, K., Bivins, A., O'Brien, J.W., Choi, P.M., Kitajima, M., Simpson, S.L., Li, J. and Tscharke, B., 2020. First confirmed detection of SARS-CoV-2 in untreated wastewater in Australia: a proof of concept for the wastewater surveillance of COVID-19 in the community. Science of the Total Environment, 728, p.138764.

Altschul, S.F., Gish, W., Miller, W., Myers, E.W. and Lipman, D.J., 1990. Basic local alignment search tool. Journal of molecular biology, 215(3), pp.403-410.

Alygizakis, N., Markou, A.N., Rousis, N.I., Galani, A., Avgeris, M., Adamopoulos, P.G., Scorilas, A., Lianidou, E.S., Paraskevis, D., Tsiodras, S. and Tsakris, A., 2020. Analytical methodologies for the detection of SARS-CoV-2 in wastewater: Protocols and future perspectives. TrAC Trends in Analytical Chemistry, p.116125.

Cao, Y., Raith, M.R. and Griffith, J.F., 2015. Droplet digital PCR for simultaneous quantification of general and human-associated fecal indicators for water quality assessment. water research, 70, pp.337-349.

Carrillo-Reyes, J., Barragán-Trinidad, M. and Buitrón, G., 2020. Surveillance of SARS-CoV-2 in sewage and wastewater treatment plants in Mexico. Journal of Water Process Engineering, p.101815.

medRxiv preprint doi: https://doi.org/10.1101/2021.03.02.21252754; this version posted January 13, 2022. The copyright holder for this preprint (which was not certified by peer review) is the author/funder, who has granted medRxiv a license to display the preprint in perpetuity. It is made available under a CC-BY-NC-ND 4.0 International license .

Cervantes-Avilés, P., Moreno-Andrade, I. and Carrillo-Reyes, J., 2021. Approaches applied to detect SARS-CoV-2 in wastewater and perspectives post-COVID-19. Journal of Water Process Engineering, p.101947.

Chu, D.K., Pan, Y., Cheng, S.M., Hui, K.P., Krishnan, P., Liu, Y., Ng, D.Y., Wan, C.K., Yang, P., Wang, Q. and Peiris, M., 2020. Molecular diagnosis of a novel coronavirus (2019-nCoV) causing an outbreak of pneumonia. Clinical chemistry, 66(4), pp.549-555.

Corman, V.M., Landt, O., Kaiser, M., Molenkamp, R., Meijer, A., Chu, D.K., Bleicker, T., Brünink, S., Schneider, J., Schmidt, M.L. and Mulders, D.G., 2020. Detection of 2019 novel coronavirus (2019-nCoV) by real-time RT-PCR. Eurosurveillance, 25(3), p.2000045.

D'Aoust, P.M., Mercier, E., Montpetit, D., Jia, J.J., Alexandrov, I., Neault, N., Baig, A.T., Mayne, J., Zhang, X., Alain, T. and Langlois, M.A., 2021. Quantitative analysis of SARS-CoV-2 RNA from wastewater solids in communities with low COVID-19 incidence and prevalence. Water research, 188, p.116560.

Dong, E., Du, H. and Gardner, L., 2020. An interactive web-based dashboard to track COVID-19 in real time. The Lancet infectious diseases, 20(5), pp.533-534.

medRxiv preprint doi: https://doi.org/10.1101/2021.03.02.21252754; this version posted January 13, 2022. The copyright holder for this preprint (which was not certified by peer review) is the author/funder, who has granted medRxiv a license to display the preprint in perpetuity. It is made available under a CC-BY-NC-ND 4.0 International license .

322 Falzone, L., Musso, N., Gattuso, G., Bongiorno, D., Palermo, C.I., Scalia, G., Libra, M. and Stefani,
323 S., 2020. Sensitivity assessment of droplet digital PCR for SARS-CoV-2 detection. International
324 journal of molecular medicine, 46(3), pp.957-964.
325
326 Forés, E., Bofill-Mas, S., Itarte, M., Martínez-Puchol, S., Hundesa, A., Calvo, M., Borrego, C.M.,
327 Corominas, L.L., Girones, R. and Rusiñol, M., 2021. Evaluation of two rapid ultrafiltration-based
328 methods for SARS-CoV-2 concentration from wastewater. Science of The Total Environment,
329 768, p.144786.
330
331 Gerrity, D., Papp, K., Stoker, M., Sims, A. and Frehner, W., 2021. Early-pandemic wastewater
332 surveillance of SARS-CoV-2 in Southern Nevada: Methodology, occurrence, and
333 incidence/prevalence considerations. Water research X, 10, p.100086.
334
335 Gonzalez, R., Curtis, K., Bivins, A., Bibby, K., Weir, M.H., Yetka, K., Thompson, H., Keeling, D.,
336 Mitchell, J. and Gonzalez, D., 2020. COVID-19 surveillance in Southeastern Virginia using
337 wastewater-based epidemiology. Water research, 186, p.116296.
338
339 Graham, K.E., Loeb, S.K., Wolfe, M.K., Catoe, D., Sinnott-Armstrong, N., Kim, S., Yamahara, K.M.,
340 Sassoubre, L.M., Mendoza Grijalva, L.M., Roldan-Hernandez, L. and Langenfeld, K., 2020. SARS-
341 CoV-2 RNA in Wastewater Settled Solids Is Associated with COVID-19 Cases in a Large Urban
342 Sewershed. Environmental science & technology.
343

medRxiv preprint doi: https://doi.org/10.1101/2021.03.02.21252754; this version posted January 13, 2022. The copyright holder for this preprint
(which was not certified by peer review) is the author/funder, who has granted medRxiv a license to display the preprint in perpetuity.
It is made available under a CC-BY-NC-ND 4.0 International license .

344 Hata, A., Hara-Yamamura, H., Meuchi, Y., Imai, S. and Honda, R., 2021. Detection of SARS-CoV-2
345 in wastewater in Japan during a COVID-19 outbreak. Science of The Total Environment, 758,
346 p.143578.
347
348 Liu, X., Feng, J., Zhang, Q., Guo, D., Zhang, L., Suo, T., Hu, W., Guo, M., Wang, X., Huang, Z. and
349 Xiong, Y., 2020. Analytical comparisons of SARS-COV-2 detection by qRT-PCR and ddPCR with
350 multiple primer/probe sets. Emerging microbes & infections, 9(1), pp.1175-1179.
351
352 Lu, X., Wang, L., Sakthivel, S.K., Whitaker, B., Murray, J., Kamili, S., Lynch, B., Malapati, L., Burke,
353 S.A., Harcourt, J. and Tamin, A., 2020. US CDC real-time reverse transcription PCR panel for
354 detection of severe acute respiratory syndrome coronavirus 2. Emerging infectious diseases,
355 26(8), p.1654.
356
357 Medema, G., Heijnen, L., Elsinga, G., Italiaander, R. and Brouwer, A., 2020. Presence of SARS-
358 Coronavirus-2 RNA in sewage and correlation with reported COVID-19 prevalence in the early
359 stage of the epidemic in the Netherlands. Environmental Science & Technology Letters, 7(7),
360 pp.511-516.
361
362 National Institute for Viral Disease Control and Prevention. Specific primers and probes for
363 detection of 2019 novel coronavirus (2020);
364 http://ivdc.chinacdc.cn/kyjz/202001/t20200121_211337.html
365

medRxiv preprint doi: https://doi.org/10.1101/2021.03.02.21252754; this version posted January 13, 2022. The copyright holder for this preprint (which was not certified by peer review) is the author/funder, who has granted medRxiv a license to display the preprint in perpetuity. It is made available under a CC-BY-NC-ND 4.0 International license .

366 Oliveira, M.D.L.A., Campos, A., Matos, A.R., Rigotto, C., Martins, A.S., Teixeira, P.F. and Siqueira,
367 M.M., 2020. Wastewater-Based Epidemiology (WBE) and Viral Detection in Polluted Surface
368 Water: A Valuable Tool for COVID-19 Surveillance—A Brief Review.
369
370 Pecson, B.M., Darby, E., Haas, C., Amha, Y., Bartolo, M., Danielson, R., Dearborn, Y., Di Giovanni,
371 G., Ferguson, C., Fevig, S. and Gaddis, E., 2021. Reproducibility and sensitivity of 36 methods to
372 quantify the SARS-CoV-2 genetic signal in raw wastewater: findings from an interlaboratory
373 methods evaluation in the US. Environmental Science: Water Research & Technology.
374
375 Prado, T., Fumian, T.M., Mannarino, C.F., Resende, P.C., Motta, F.C., Eppinghaus, A.L.F., do Vale,
376 V.H.C., Braz, R.M.S., de Andrade, J.D.S.R., Maranhão, A.G. and Miagostovich, M.P., 2021.
377 Wastewater-based epidemiology as a useful tool to track SARS-CoV-2 and support public health
378 policies at municipal level in Brazil. Water research, 191, p.116810.
379
380 Rački, N., Morisset, D., Gutierrez-Aguirre, I. and Ravnikar, M., 2014. One-step RT-droplet digital
381 PCR: a breakthrough in the quantification of waterborne RNA viruses. Analytical and
382 bioanalytical chemistry, 406(3), pp.661-667.
383
384 Randazzo, W., Cuevas-Ferrando, E., Sanjuán, R., Domingo-Calap, P. and Sánchez, G., 2020.
385 Metropolitan wastewater analysis for COVID-19 epidemiological surveillance. International
386 Journal of Hygiene and Environmental Health, 230, p.113621.
387

medRxiv preprint doi: https://doi.org/10.1101/2021.03.02.21252754; this version posted January 13, 2022. The copyright holder for this preprint
(which was not certified by peer review) is the author/funder, who has granted medRxiv a license to display the preprint in perpetuity.
It is made available under a CC-BY-NC-ND 4.0 International license .

388 Sarmila, T., Sherchan, S.P. and Eiji, H., 2020. Applicability of crAssphage, pepper mild mottle
389 virus, and tobacco mosaic virus as indicators of reduction of enteric viruses during wastewater
390 treatment. Scientific Reports (Nature Publisher Group), 10(1).
391
392 Sherchan, S.P., Shahin, S., Ward, L.M., Tandukar, S., Aw, T.G., Schmitz, B., Ahmed, W. and
393 Kitajima, M., 2020. First detection of SARS-CoV-2 RNA in wastewater in North America: a study
394 in Louisiana, USA. Science of The Total Environment, 743, p.140621.
395
396 Suo, T., Liu, X., Feng, J., Guo, M., Hu, W., Guo, D., Ullah, H., Yang, Y., Zhang, Q., Wang, X. and
397 Sajid, M., 2020. ddPCR: a more accurate tool for SARS-CoV-2 detection in low viral load
398 specimens. Emerging microbes & infections, 9(1), pp.1259-1268.
399
400 Torii, S., Furumai, H. and Katayama, H., 2021. Applicability of polyethylene glycol precipitation
401 followed by acid guanidinium thiocyanate-phenol-chloroform extraction for the detection of
402 SARS-CoV-2 RNA from municipal wastewater. Science of The Total Environment, 756, p.143067.
403
404 Worley-Morse, T., Mann, M., Khunjar, W., Olabode, L. and Gonzalez, R., 2019. Evaluating the
405 fate of bacterial indicators, viral indicators, and viruses in water resource recovery facilities.
406 Water Environment Research, 91(9), pp.830-842.
407

medRxiv preprint doi: https://doi.org/10.1101/2021.03.02.21252754; this version posted January 13, 2022. The copyright holder for this preprint
(which was not certified by peer review) is the author/funder, who has granted medRxiv a license to display the preprint in perpetuity.
It is made available under a CC-BY-NC-ND 4.0 International license .

408 Yang, R., Paparini, A., Monis, P. and Ryan, U., 2014. Comparison of next-generation droplet
409 digital PCR (ddPCR) with quantitative PCR (qPCR) for enumeration of Cryptosporidium oocysts
410 in faecal samples. International journal for parasitology, 44(14), pp.1105-1113.

411

412

medRxiv preprint doi: https://doi.org/10.1101/2021.03.02.21252754; this version posted January 13, 2022. The copyright holder for this preprint
(which was not certified by peer review) is the author/funder, who has granted medRxiv a license to display the preprint in perpetuity.
It is made available under a CC-BY-NC-ND 4.0 International license .

413 **Figures/Tables**

414

415 Figure 1. Locations of RT-ddPCR and RT-qPCR designed assays with respect to the SARS-CoV-2

416 genome (GenBank accession no. MN908947). ddCoV_N and nCoV_N2 assays are located on the

417 N gene (top panel). ddCoV_E and E_Sarbeco are located on the E gene (bottom panel).

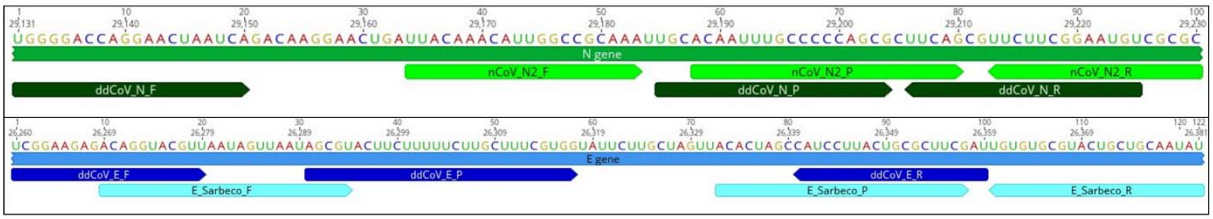

418
419

medRxiv preprint doi: https://doi.org/10.1101/2021.03.02.21252754; this version posted January 13, 2022. The copyright holder for this preprint
(which was not certified by peer review) is the author/funder, who has granted medRxiv a license to display the preprint in perpetuity.
It is made available under a CC-BY-NC-ND 4.0 International license .

420 Figure 2. Annealing temperature thermal gradient optimizations for the 2 RT-ddPCR designed
421 assays (ddCoV_N, ddCoV_E) and the 2 RT-qPCR designed assays (nCoV_N2, E_Sarbeco). Thicker
422 portion of the positive band (first 8 wells) used RNA oligo standard, while the thinner portion
423 (next 8 wells) used a SARS-CoV-2 positive wastewater sample. The last 8 wells are negatives
424 (NTC).
425

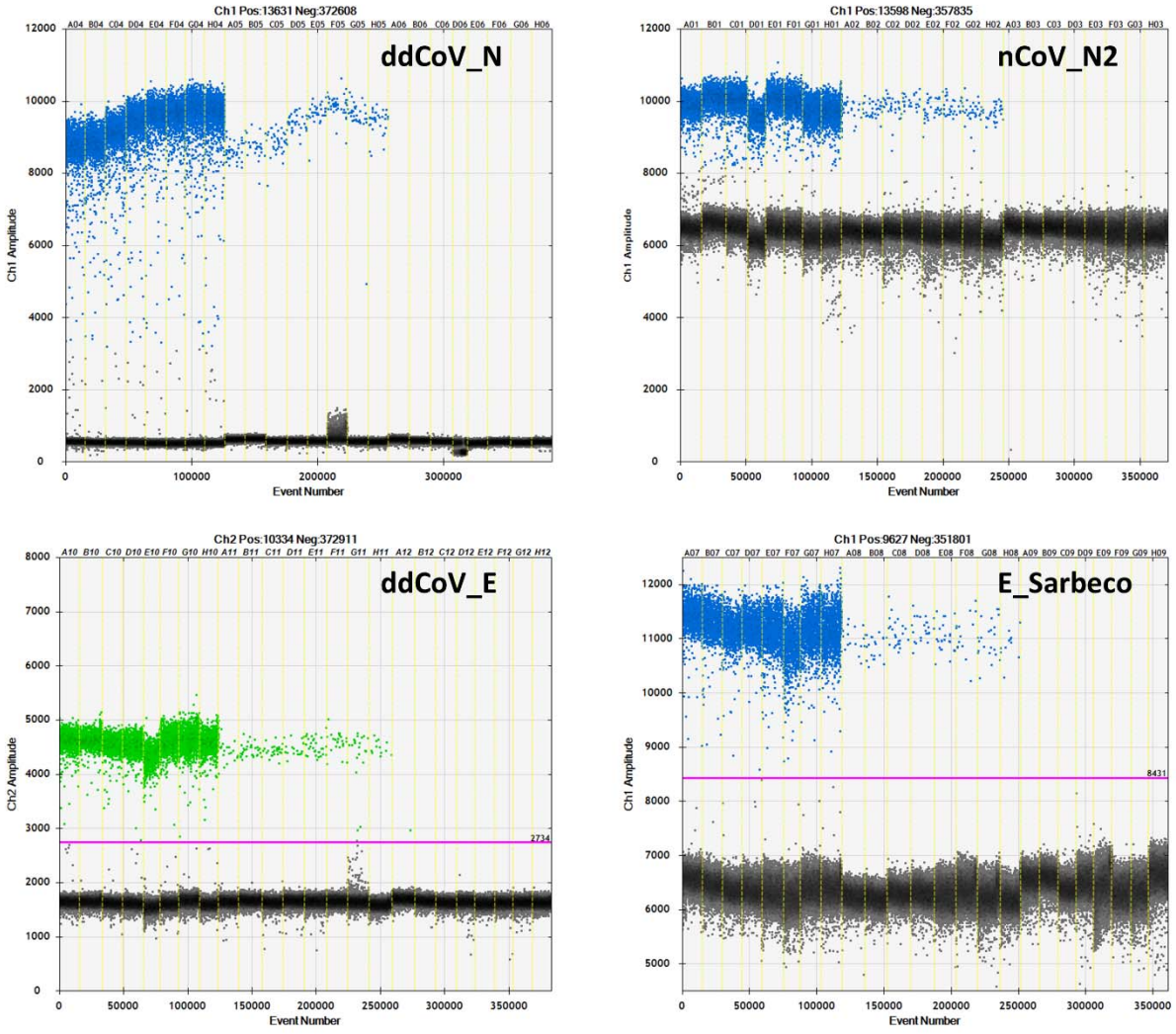

426

medRxiv preprint doi: https://doi.org/10.1101/2021.03.02.21252754; this version posted January 13, 2022. The copyright holder for this preprint
(which was not certified by peer review) is the author/funder, who has granted medRxiv a license to display the preprint in perpetuity.
It is made available under a CC-BY-NC-ND 4.0 International license .

427 Figure 3. ddCoV_N and ddCoV_E positive droplets and copies per reaction for the limits of

428 detection serial dilutions. Coefficients of variation (CV) for the copies per reaction are shown.

429

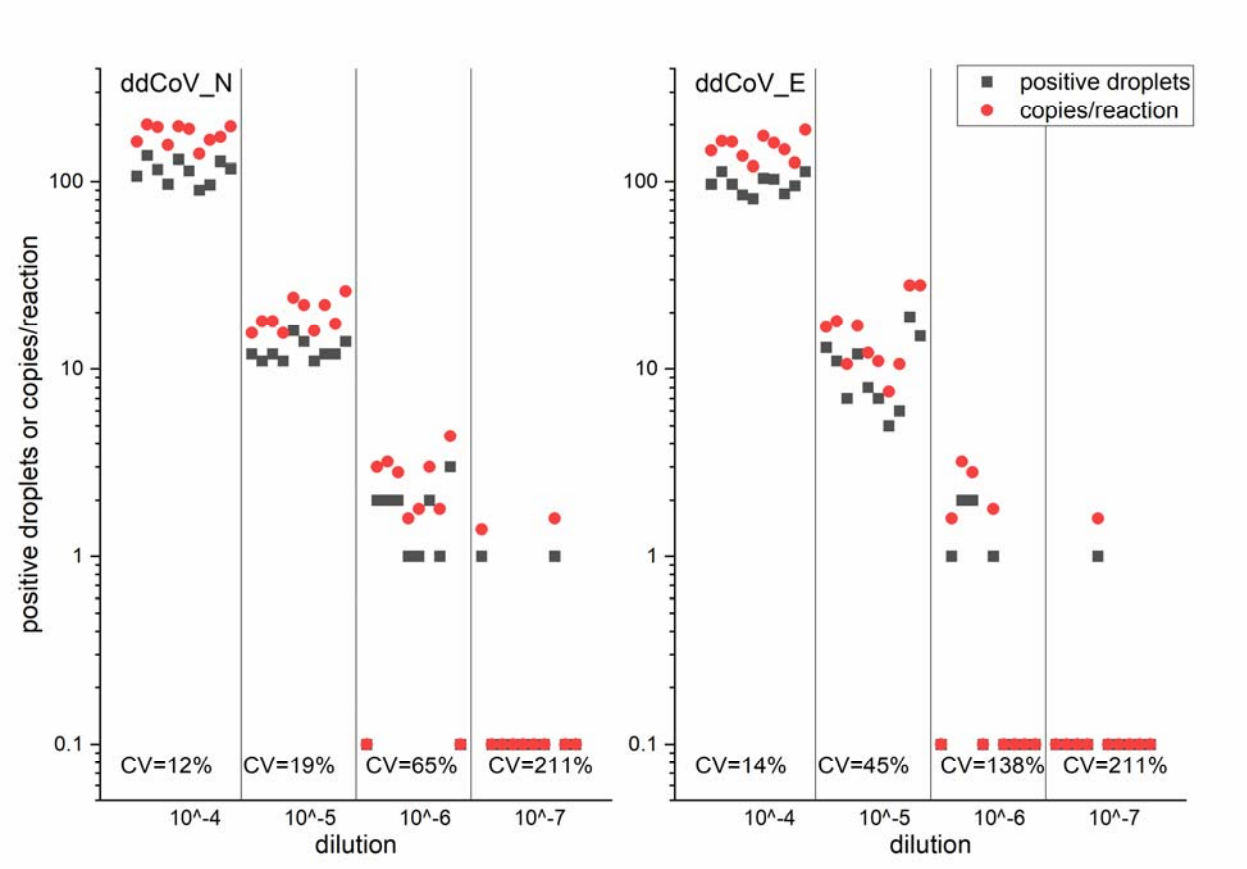

430

medRxiv preprint doi: https://doi.org/10.1101/2021.03.02.21252754; this version posted January 13, 2022. The copyright holder for this preprint
(which was not certified by peer review) is the author/funder, who has granted medRxiv a license to display the preprint in perpetuity.
It is made available under a CC-BY-NC-ND 4.0 International license .

431 Figure 4. Assay comparisons for three weeks of wastewater SARS-CoV-2 concentrations at 9

432 facilities in southeast Virginia. Only the detectable concentrations are shown (N=26).

433

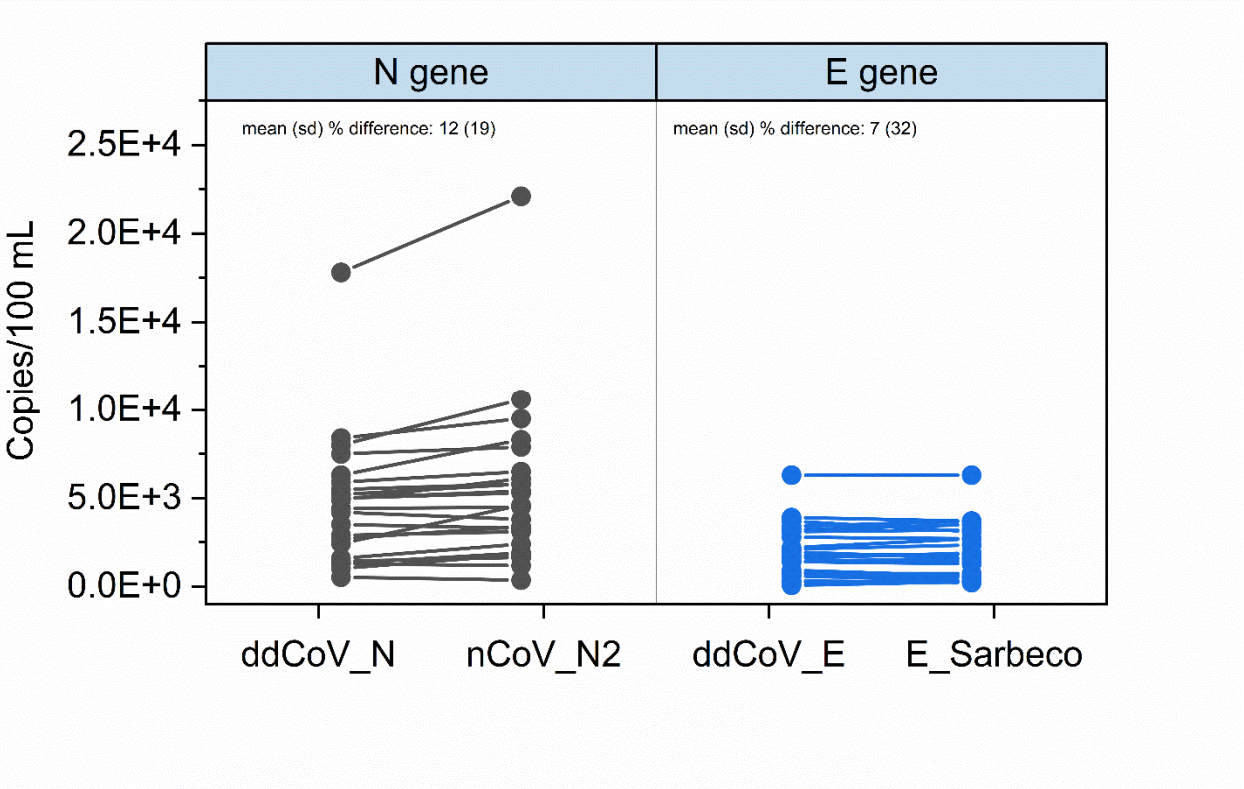

434

medRxiv preprint doi: https://doi.org/10.1101/2021.03.02.21252754; this version posted January 13, 2022. The copyright holder for this preprint
(which was not certified by peer review) is the author/funder, who has granted medRxiv a license to display the preprint in perpetuity.
It is made available under a CC-BY-NC-ND 4.0 International license .

435 Figure 5. The 2-D plot of the ddCoV_N and ddCoV_E multiplexed assays for the first 9 samples

436 analyzed. Efficient clustering of the droplet populations is shown—gray = double negative, blue

437 = FAM positive, green = HEX positive, and orange = double positive.

438

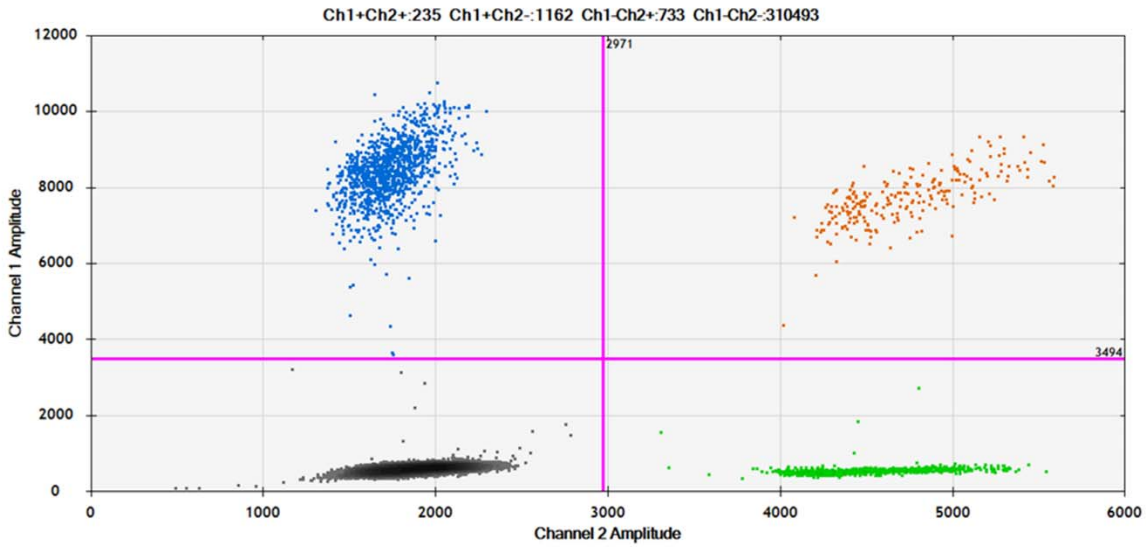

439

medRxiv preprint doi: https://doi.org/10.1101/2021.03.02.21252754; this version posted January 13, 2022. The copyright holder for this preprint (which was not certified by peer review) is the author/funder, who has granted medRxiv a license to display the preprint in perpetuity. It is made available under a CC-BY-NC-ND 4.0 International license .

440 Table 1. The N and E gene primer/probe sequences designed for RT-ddPCR. Genome locations

441 based on SARS-CoV-2 (GenBank accession no. MN908947).

442

	Sequence (5'-3')	Genome Location	Amplicon Length
ddCoV_N			95
forward	TGGGGACCAGGAACTAATCA	20131-29150	
reverse	ACATTCCGAAGAACGCTGAA	29225-29206	
probe	FAM/TGCACAATT/ZEN/TGCCCCCAGCG/IABkFQ	29185-29204	
ddCoV_E			100
forward	TCGGAAGAGACAGGTACGTT	26260-26279	
reverse	ATCGAAGCGCAGTAAGGATG	26359-26340	
probe	HEX/AGCGTACTT/ZEN/CTTTTTCTTGCTTTCGTGG/IABkFQ	26290-26317	

443

medRxiv preprint doi: https://doi.org/10.1101/2021.03.02.21252754; this version posted January 13, 2022. The copyright holder for this preprint
(which was not certified by peer review) is the author/funder, who has granted medRxiv a license to display the preprint in perpetuity.
It is made available under a CC-BY-NC-ND 4.0 International license .

444 Table 2. Primer and probe sequence information. Sequences with an asterisk (*) exhibits high

445 end self complementarity.

446

	Tm (°C)	GC (%)	ANY	SELF
ddCoV_N				
probe	66.8	60	6	2
forward	60	50	3	2
reverse	60.1	45	5	0
ddCoV_E				
probe	66.9	42.9	4	0
forward	60.4	50	4	2
reverse	60.4	50	4	0
nCoV_N2				
probe	68.8	56.5	6	2
forward*	59.4	40	5	5
reverse	60.7	55.6	5	2
E_Sarbeco				
probe	69.1	53.8	4	2
forward*	60.6	34.6	8	8
reverse	63.2	45.5	7	1

447